Article

Beyond Two-State Conical Intersections. Three-State Conical Intersections in Low Symmetry Molecules: the Allyl Radical

Spiridoula Matsika, and David R. Yarkony

J. Am. Chem. Soc., **2003**, 125 (35), 10672-10676• DOI: 10.1021/ja036201v • Publication Date (Web): 08 August 2003

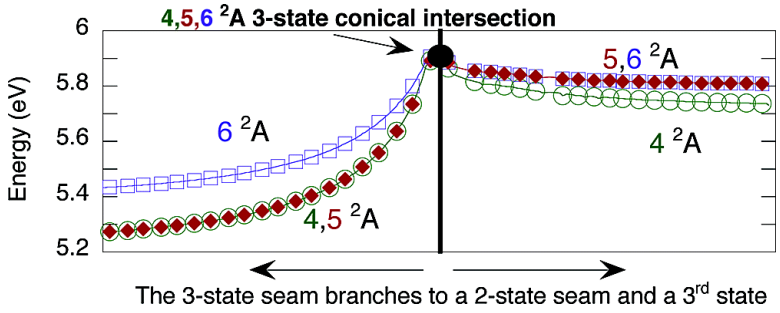

More About This Article

Additional resources and features associated with this article are available within the HTML version:

- Supporting Information
- Links to the 5 articles that cite this article, as of the time of this article download
- Access to high resolution figures
- Links to articles and content related to this article
- Copyright permission to reproduce figures and/or text from this article

View the Full Text HTML

J|A|C|S
ARTICLES
Published on Web 08/08/2003

Beyond Two-State Conical Intersections. Three-State Conical Intersections in Low Symmetry Molecules: the Allyl Radical

Spiridoula Matsika* and David R. Yarkony*

Contribution from the Department of Chemistry, Johns Hopkins University, Baltimore, Maryland 21218

Received May 16, 2003; E-mail: smatsika@jhu.edu; yarkony@jhu.edu

Abstract: Using multireference configuration interaction expansions comprised of over 7 million configuration state functions, three-state conical intersections are reported for the closely spaced, spectroscopically observed $\tilde{B}(^2A_1)$, $\tilde{C}(^2B_1)$, and $\tilde{D}(^2B_2)$ states (in C_{2v} symmetry) of the allyl radical. These conical intersections of states which were previously assigned as the $3,4,5^2A$ states and are here reassigned as the $4,5,6^2A$ states, are expected to be accessible using optical probes. This conclusion is obtained from the structure of the minimum energy point on the $4,5,6^2A$ three-state conical intersection seam which is similar to the equilibrium structure of the ground $\tilde{X}(^2A_2)$ state and only 1.1 eV above the $\tilde{D}(^2B_2)$ state at its equilibrium geometry. The seam of three-state degeneracies joins two two-state seams of conical intersection, the $4,5^2A$ and $5,6^2A$ conical intersection seams. The energy of the minimum energy point on the $4,5^2A$ two-state seam is only 0.15 eV above that of the $\tilde{D}(^2B_2)$ state at its equilibrium structure. Three-state intersections are also reported for the $3,4,5^2A$ states.

1. Introduction

It is now well established that conical intersections of two states of the same symmetry play a key role in the nonadiabatic radiationless decay of electronically excited states.[1−3] For molecules with no spatial symmetry and four or more atoms, conical intersections of three states are also possible.

Three-state intersections may play a role in nonadiabatic processes involving several electronic states. Collisions of ground-state moieties at hyperthermal energies can produce excited electronic states of the products requiring more than one "upward" nonadiabatic transition. Conversely, photodissociation can involve excitation of a bright state, followed by electronic cascade through lower (dark) electronic states to the ground electronic state. It is reasonable to describe such processes as a sequence of two-state nonadiabatic transitions, each of which is facilitated by a seam of two-state conical intersections. While such a sequence of pairwise nonadiabatic transitions can be quite efficient, this need not be the case. For the consecutive adiabatic states i, j, and k, the downward sequence, $k \rightarrow j \rightarrow i$, will be compromised if the k, j conical intersection routes the molecule away from the region of the j, i conical intersection. The situation is further complicated in an upward sequence of nonadiabatic transitions since a conical intersection can deflect a (slowly moving) wave packet from the conical intersection region. The impact of these bottlenecks can be mitigated if multistate nonadiabatic transitions are possible. Conical intersections of three electronic states are clearly germane in this regard. Indeed, it was a near intersection of three states relevant to the nonadiabatic reaction $O(^3P) + H_2O \rightarrow OH(X) + OH(A)$ that motivated our work in this area.[4]

Three-state conical intersections required by symmetry have long been studied in the context of the Jahn−Teller problem.[5] The three-state intersections considered here,[6,7] which do not depend on symmetry, have received little attention although they are potentially quite interesting. The branching space[8] for these conical intersections, the space in which the double cone topography is evinced, is five dimensional[7] and connects each electronic state with two other states. This should be contrasted with two-state conical intersections, with a two-dimensional branching space connecting only a single pair of electronic states.

The limited attention paid to three-state conical intersections is due in part to the low dimension of the degeneracy or seam space, which is $N^{\text{int}} - 5$, where N^{int} is the number of internal coordinates. This makes three-state conical intersections difficult to locate. Recently, we have reported an algorithm that removes this obstacle to their study.[9] This algorithm uses analytic gradient and Lagrange multiplier, techniques to efficiently locate conical intersections of three electronic states whose description is based on extended multireference configuration interaction (MRCI) wave functions.

The photodissociation dynamics of organic radicals relevant to combustion processes, including ethyl,[10] propargyl,[11,12] hy-

(1) Robb, M. A.; Garavelli, M.; Olivucci, M.; Bernardi, F. *Rev. Comput. Chem.* **2000**, *15*, 87.
(2) Yarkony, D. R. *J. Phys. Chem. A* **2001**, *105*, 6277−6293.
(3) Klessinger, M.; Michl, J. *Excited States and Photochemistry of Organic Molecules*; VCH Publishers: New York, 1995.
(4) Matsika, S.; Yarkony, D. R. *J. Chem. Phys.* **2002**, *117*, 3733−3740.
(5) Bersuker, I. B. *The Jahn−Teller Effect and Vibronic Interactions in Modern Chemistry*; Plenum Press: New York and London, 1984.
(6) Katriel, J.; Davidson, E. R. *Chem. Phys. Lett.* **1980**, *76*, 259−262.
(7) Keating, S. P.; Mead, C. A. *J. Chem. Phys.* **1985**, *82*, 5102−5117.
(8) Atchity, G. J.; Xantheas, S. S.; Ruedenberg, K. *J. Chem. Phys.* **1991**, *95*, 1862.
(9) Matsika, S.; Yarkony, D. R. *J. Chem. Phys.* **2002**, *117*, 6907.
(10) Gilbert, T.; Grebner, T.; Fischer, I.; Chen, P. *J. Chem. Phys.* **1999**, *110*, 5485.

10.1021/ja036201v CCC: $25.00

droxymethyl,[13,14] vinoxy,[15−17] and allyl,[18−20] continues to be an area of active research. The allyl radical is of particular interest here as it has three very closely spaced excited states at 5.1 ± 0.1 eV,[21] the $\tilde{B}(^2A_1)$, $\tilde{C}(^2B_1)$, and $\tilde{D}(^2B_2)$ states in C_{2v} symmetry. Although the allyl radical is discussed in many organic chemistry textbooks as the simplest unsaturated radical, the details of its electronically excited states remain to be clarified. Recent experimental studies of its electronic spectrum and photodissociation dynamics[19−26] have raised questions concerning the coupling of the $\tilde{B}(^2A_1)$, $\tilde{C}(^2B_1)$, and $\tilde{D}(^2B_2)$ states. Theoretical treatments using a small configuration interaction (CI) expansion[27] or a spin-coupled valence bond based CI[28] have reported vertical excitation energies for both valence and Rydberg states but have not addressed either the question of interstate interactions or the existence of conical intersections. A survey of previous calculations is given by Oliva et al.[28]

In this work we consider whether three-state conical intersections exist in the allyl radical and, if so, under what conditions they might impact photodissociation involving the $\tilde{B}(^2A_1)$, $\tilde{C}(^2B_1)$, and $\tilde{D}(^2B_2)$ states. Section 2 outlines our MRCI treatment of the six lowest electronic states. Section 3 presents the results of this study. In that section, the $\tilde{B}$, $\tilde{C}$, and $\tilde{D}$ states at 5 eV, previously assigned as the $3,4,5^2A$ states (using no symmetry designations), are reassigned to the $4,5,6^2A$ states, and three-state intersections of the $3,4,5^2A$ and $4,5,6^2A$ states are reported and analyzed. In a previous study, we have reported three-state conical intersections corresponding to the three Rydberg 3p states in the ethyl radical.[9] While a significant finding, that three-state intersection is in a sense less challenging than either the $3,4,5^2A$ or $4,5,6^2A$ conical intersections reported here. For the $3,4,5^2A$ conical intersection, the degenerate states are predominantly linear combinations of "in plane" 3s−3p hybrid Rydberg functions on the three carbons. Therefore, it represents a generalization of the well-known ^2A, ^2E triple degeneracy in H_3 to the low symmetry case. The $4,5,6^2A$ conical intersection is a 3s−3p Rydberg type intersection involving two "in-plane" 3s−3p hybrid orbitals and an "out of plane" $3p_z$ Rydberg orbital. Section 4 summarizes and describes directions for future research.

2. Theoretical Approach

The states of interest in this work have either valence character, formed from three π carbon orbitals (a_2, b_1, b_1 in C_{2v} symmetry), or Rydberg character, formed from linear combinations of diffuse 3s and 3p functions on carbon. To adequately describe all these states, the molecular orbitals were expanded in terms of a polarized Gaussian double-ζ basis set on hydrogen and carbon,[29] with the carbon basis augmented with two s and one p diffuse functions,[30] giving a (6s, 3p, 1d) basis on carbon. The molecular orbitals were obtained from a six-state, state averaged MCSCF calculation. The wave functions were constructed from a split active space, AS1 + AS2, with AS1 consisting of the three carbon π orbitals and AS2 consisting of four Rydberg orbitals. The active space expansion, used in both the MCSCF and MRCI procedures, consisted of all configuration state functions (CSFs) obtained from distributing (3,0) and (2,1) electrons in (AS1,AS2). Two different MRCI expansions, denoted CI1 and CI2, were used. In each case, the three carbon 1s orbitals were kept doubly occupied. CI1 is a quasi first-order CI expansion, consisting of the above-noted active space expansion plus all singly excited CSFs, while CI2 is a quasi second-order expansion, comprised of 7 021 882 CSFs, which included CI1 plus all doubly excited CSFs consistent with the interacting space[31] restriction. Two- and three-state conical intersections and single potential energy surface minima were determined using CI1 and CI2. The three-state conical intersections were located using the previously reported analytic gradient based algorithm noted above.[9] Calculations were done with a pre-release version of the COLUMBUS[32,33] suite of programs in which the algorithms for locating conical intersections have been included. These algorithms will be included in a future release of COLUMBUS.

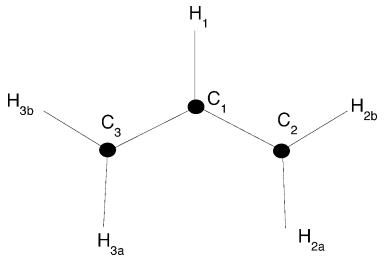

Figure 1. Equilibrium structure of the allyl radical in its ground state and labeling of the atoms.

3. Discussion

In this section, geometries will be denoted by **R**. Figure 1 shows the labeling for each atom that will be used throughout this paper to define the bond distances and bond angles that constitute **R**. No symmetry indexing will be used for the states so that energies are denoted by $E_i(\mathbf{R})$, $i = 1-6$. The equilibrium structures for the six states in question, $\mathbf{R}(\text{eql}i)$, $i = 1-6$, were determined using CI1. Eql1, presented in Figure 1, was reoptimized using CI2, but the changes were insignificant. The $\mathbf{R}(\text{eql}i)$ geometries, $i = 1-6$, are presented in Table 1. The corresponding energies $E_i(\mathbf{R}(\text{eql}i))$, $i = 1-6$, determined at the CI1 level and the CI2 level using CI1 optimized geometries, are presented in Table 2. There, and throughout this work, the zero of energy is taken as $E_1(\mathbf{R}(\text{eql1})) = -116.860\,416(-116.562\,438)$ au when CI2 (CI1) is used. The excitation energies obtained from CI2 increase by about 0.2 eV when compared with the CI1 results. This is not entirely unexpected since differential electron correlation effects are expected to be more important in the more compact ground state than the Rydberg states. In this regard, note that, in Table 2, the change in

(11) Deyerl, H.-J.; Fischer, I.; Chen, P. *J. Chem. Phys.* **1999**, *111*, 3441.
(12) Gilbert, T.; Pfab, R.; Fischer, I.; Chen, P. *J. Chem. Phys.* **2000**, *112*, 2575.
(13) Conroy, D.; Aristov, V.; Feng, L.; Reisler, H. *J. Phys. Chem. A* **2000**, *104*, 10288.
(14) Hoffman, B.; Yarkony, D. R. *J. Chem. Phys.* **2002**, *116*, 8300.
(15) Osborn, D. L.; Choi, H.; Mordaunt, D. H.; Bise, R. T.; Neumark, D. M.; Rohlfing, C. M. *J. Chem. Phys.* **1997**, *106*, 3049−3066.
(16) Brock, L. R.; Rohlfing, E. A. *J. Chem. Phys.* **1997**, *106*, 10048−10065.
(17) Matsika, S.; Yarkony, D. R. *J. Chem. Phys.* **2002**, *117*, 7198.
(18) Deyerl, H.-J.; Fischer, I.; Chen, P. *J. Chem. Phys.* **1999**, *110*, 1450.
(19) Gilbert, T.; Fischer, I.; Chen, P. *J. Chem. Phys.* **2000**, *113*, 561.
(20) Getty, J. D.; Liu, S.; Kelly, P. B. *J. Phys. Chem.* **1992**, *96*, 10155.
(21) Blush, J. A.; Minsek, D. W.; Chen, P. *J. Phys. Chem.* **1992**, *96*, 10150.
(22) Hudgens, J. W.; Dulcey, C. S. *J. Phys. Chem.* **1985**, *89*, 1505.
(23) Sappey, A. D.; Weisshaar, J. C. *J. Phys. Chem.* **1987**, *91*, 3731.
(24) Minsek, D. W.; Chen, P. *J. Phys. Chem.* **1993**, *97*, 13375.
(25) Schultz, T.; Fischer, I. *J. Chem. Phys.* **1998**, *109*, 5812.
(26) Wu, J.; Li, R.; Chang, J.; Chen, Y. *J. Chem. Phys.* **2000**, *113*, 7286.
(27) Ha, T.-K.; Baumann, H.; Oth, J. F. M. *J. Chem. Phys.* **1986**, *85*, 1438.
(28) Oliva, J. M.; Gerratt, J.; Cooper, D. L.; Karadakov, P. B.; Raimondi, M. *J. Chem. Phys.* **1997**, *106*, 3663.
(29) Dunning, T. H.; *J. Chem. Phys.* **1970**, *53*, 2823.
(30) Dunning, T. H., Jr.; Hay, P. J. Gaussian basis sets for molecular calculations; In *Methods of Electronic Structure Theory*; Schaefer, H. F., III., Ed.; Plenum Press: New York and London, 1977; pp 1−27.
(31) McLean, A. D.; Liu, B. *J. Chem. Phys.* **1973**, *58*, 1066.
(32) Shepard, R.; Shavitt, I.; Pitzer, R. M.; Comeau, D. C.; Pepper, M.; Lischka, H.; Szalay, P. G.; Ahlrichs, R.; Brown, F. B.; Zhao, J. *Int. J. Quantum Chem., Quantum Chem. Symp.* **1988**, *22*, 149.
(33) For information on the COLUMBUS programs, see: www.itc.univie.ac.at/hans/Columbus/columbus.html.

Table 1. Geometries at the Minima of the Six Lowest States and at the Conical Intersections[a]

	1^2A	2^2A	3^2A	4^2A	5^2A	6^2A	$4,5,6^2A$	$3,4,5^2A$	$4,5^2A$	$5,6^2A$
$R(C_1-C_2)$	1.397	1.462	1.392	1.390	1.394	1.392	1.410	1.405	1.411	1.395
$R(C_1-C_3)$	1.397	1.462	1.392	1.390	1.394	1.392	1.441	1.412	1.410	1.397
$R(C_1-H_1)$	1.091	1.090	1.084	1.10	1.087	1.087	1.078	1.382	1.063	1.084
$R(C_2-H_{2a})$	1.088	1.086	1.088	1.094	1.092	1.089	1.069	1.192	1.101	1.100
$R(C_2-H_{2b})$	1.086	1.086	1.090	1.088	1.088	1.087	1.098	1.088	1.098	1.094
$R(C_3-H_{3a})$	1.088	1.086	1.088	1.094	1.092	1.087	1.098	1.185	1.100	1.134
$R(C_3-H_{3b})$	1.086	1.086	1.090	1.088	1.088	1.087	1.081	1.089	1.098	1.087
$\angle C_2C_1C_3$	124.9	123.3	119.4	117.6	118.8	119.2	123.5	108.9	123.8	122.1
$\angle C_1C_2H_{2a}$	121.0	120.4	121.1	120.8	121.1	120.7	118.3	118.4	122.9	117.9
$\angle C_1C_2H_{2b}$	121.0	120.4	121.0	120.6	121.7	121.2	122.6	128.5	125.8	125.3
$\angle H_1C_1C_2$	117.5	118.4	120.3	121.2	120.6	120.4	116.2	125.8	117.7	122.4
$\angle C_1C_2C_3H_1$		0.1					180	180	177	177.4
$\angle H_1C_1C_2H_{2a}$		203.4					220.6	137.7	177.2	223.0
$\angle H_1C_1C_2H_{2b}$		30					46.7	327.3	358.7	56
$\angle H_1C_1C_3H_{3a}$		203					136.1	135.8	176.2	150.9
$\angle H_1C_1C_3H_{3b}$		30					339.9	330.5	4.9	10
$\angle C_1C_2H_{2a}H_{2b}$		186.1					5.9	8.1	1.3	11.6
$\angle C_1C_3H_{3a}H_{3b}$		174					22.2	13.0	7.7	19.6

[a] The geometries at the equilibrium points are calculated using the CI1 expansion and at the conical intersections using the CI2 expansion. Bond lengths are given in angstrom, and angles, in degrees. Dihedral angles are shown only for the nonplanar states. Experimental geometries for the ground state are as follows: $R(C_1-C_2) = 1.3869$ Å,[35] $\angle C_2C_1C_3 = 123.96$,[35] and, for the $\tilde{C}$ state, $\angle C_2C_1C_3 = 117.5$.[36]

Table 2. Excitation Energies for the Six Lowest States of the Allyl Radical and Energies at the Conical Intersections[a]

	E_2	E_3	E_4	E_5	E_6	$E_x(456)$	$E_x(345)$	$E_x(45)$	$E_x(56)$
vertical CI1	3.49	4.48	5.02	5.09	5.23				
vertical CI2	3.36	4.70	5.25	5.31	5.50				
adiabatic CI1	3.26	4.45	4.95	5.05	5.19	5.93	7.17	5.25	5.81
adiabatic CI2	3.10	4.66	5.17	5.26	5.45	6.40	7.37	5.41	6.23
Ha et al.[27]	3.13	5.33	5.86	5.26	5.52				
Oliva et al.[28]	3.19	5.12	5.70	5.78	5.73				
expt[21]	3.07		4.97	5.15	5.00				

[a] Previous theoretical and experimental results are included. Energies are given in eV.

$E_i(\mathbf{R}(\text{eql}i)) - E_1(\mathbf{R}(\text{eql1}))$, in going from CI1 to CI2, is smallest for $i = 2$ which, as discussed below, is also a valence state.

3.1. Assignment of the $\tilde{B}(^2A_1)$, $\tilde{C}(^2B_2)$, and $\tilde{D}(^2B_1)$ States. Of the six states considered, five were found to be planar and have C_{2v} symmetry. Only the $\tilde{A}$ state was found to be nonplanar having C_2 symmetry in agreement with previous work.[34] For C_{2v} geometries, these six states are the 1^2A_2, 1^2B_1, 1^2A_1, 2^2A_1, 1^2B_2, and 2^2B_1 states, respectively. At eql1, the ground state and first excited state are valence in character arising from the three π orbitals, with dominant configurations $...6a_1^2 4b_2^2 1b_1^2 1a_2^1$ and $(...6a_1^2 4b_2^2 1a_2^2 1b_1^1 + ...6a_1^2 4b_2^2 1b_1^2 2b_1^1)$, respectively. The higher-energy states are Rydberg, arising from an excitation from the a_2 orbital to any of the four Rydberg orbitals. Three of the four Rydberg states considered in this work are very close in energy, making their assignment difficult. Table 2 compares the present results with previous experimental and theoretical findings. None of the previous theoretical studies were able to reproduce the experimentally derived ordering of these states, and their predicted excitation energies are too high. The calculations reported here include more correlation than the previous studies, and as a result, the excitation energies are substantially improved. However some discrepancies remain. We find, using CI1, a $^2A_1$ state at virtually the same energy as that observed experimentally. However this state is the second, rather than the first, state of $^2A_1$ symmetry. For consistency with previous work, we label the 1^2A_1 and 2^2A_1 states as the $\tilde{B}'(^2A_1)$ and $\tilde{B}(^2A_1)$ states, respectively. The theoretical work of Oliva et al.[28] also predicts two $^2A_1$ states below the 2^2B_1, 1^2B_2 states, in agreement with the present work. However, their excitation energies are higher than ours. Ha et al.[27] report two $^2A_1$ states but at energies higher than that of 1^2B_2 states, in contradiction to all other results.

The 1^2A_1 ($\tilde{B}'(^2A_1)$) state could have easily escaped experimental detection. The electronic transition from the ground $^2A_2$ state to a $^2A_1$ state is dipole forbidden by symmetry. The experimental detection of the 2^2A_1 ($\tilde{B}(^2A_1)$) state is enabled by intensity borrowing, vibronic coupling, to the 2^2B_1 state and/or 1^2B_2 state, which are in close proximity. The 1^2A_1 ($\tilde{B}'(^2A_1)$) state on the other hand is predicted here to be approximately 0.5 eV lower than the closely spaced 2^2A_1, 2^2B_1, and 1^2B_2, states and thus is much less likely to borrow intensity from those states. This could explain why only the 2^2A_1 state has been observed.

From Table 2, it is seen that the adiabatic separation of the 2^2B_1 and 1^2B_2 states is 0.14 (0.19) eV, with the lower state 0.10 (0.09) eV above the $\tilde{B}(^2A_1)$ state, at the CI1(CI2) level. These values are in good accord with the experimental results *except* that the symmetry of the closely spaced 2^2B_1 and 1^2B_2 is the opposite of that derived from experiment. Only Oliva et al.[28] predict the 2^2B_1 state (at 5.73 eV) to be lower than the 1^2B_2 (at 5.78 eV), although the absolute and relative excitation energies suggest this agreement may be fortuitous. The first principles determination of the ordering of these states will be the subject of future work.

3.2. $4,5,6^2A$ Conical Intersections. The close proximity of the $\tilde{B}(^2A_1)$, $\tilde{C}(^2B_1)$, and $\tilde{D}(^2B_2)$ Rydberg states leads us to ask whether conical intersections involving these states exist and, if they do, whether they are accessible and relevant to the recent studies of allyl photodissociation.[18,19] Of special interest here are three-state conical intersections since there is little information available about their existence and properties in general. To address these questions, three-state, and two-state, conical intersections involving the $\tilde{B}(^2A_1)$, $\tilde{C}(^2B_1)$, and $\tilde{D}(^2B_2)$ (the $4,5,6^2A$) Rydberg states were sought. The $4,5,6^2A$ states were found to become degenerate for nonplanar structures with no spatial symmetry. Points on this three-state conical intersection

(34) Tonokura, K.; Koshi, M. *J. Phys. Chem. A* **2000**, *104*, 8456.
(35) Hirota, E.; Yamada, C.; Okunishi, M. *J. Chem. Phys.* **1992**, *97*, 2963.
(36) Minsek, D. W.; Blush, J. A.; Chen, P. *J. Phys. Chem.* **1992**, *96*, 2025.

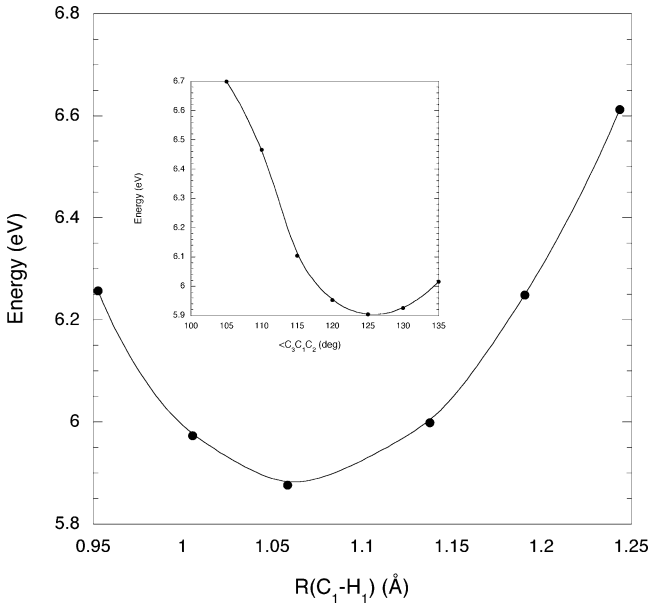

Figure 2. Seam of conical intersections between the 4,5,6^{2}A states using CI1. Energy of the three states along the R(C_1−H_1) coordinate and along the ∠$C_2C_1C_3$ coordinate in the insert figure.

seam, obtained using CI1, are shown in Figure 2 as a function of either of the internal coordinates, R(C_1−H_1) or ∠$C_3C_1C_2$, with the remaining ($N^{\text{int}} - 5 - 1$) degrees of freedom optimized to reduce the energy of the crossing. The energy at ci456, minimum energy point on this seam, $E_x(456) = E_j(\mathbf{R}(\text{ci456}))$, $j = 4, 5, 6$, is 5.9 eV, less than 0.7 eV higher than $E_6(\mathbf{R}(\text{eql1}))$, the vertical excitation energy to the 6^2A (2^2B_1) state. Here, and in the following discussion, a minimum energy point of conical intersection involving two or three states will be denoted ci{state1}{state2} or ci{state1}{state2}{state3}. The main difference between **R**(eql1) and **R**(ci456) is the loss of planar symmetry with the terminal hydrogen atoms (H_{2a},H_{2b},H_{3a},H_{3b}) rotated out of the plane in a disrotatory fashion.

To demonstrate that these three-state intersections are not an artifact of the CI1 expansion, ci456 was sought and found using CI2. Its energy and geometry are reported in Tables 2 and 1, respectively. Unlike **R**(eql1), **R**(ci456) is affected by the differences in electron correlation between CI1 and CI2. $\Delta E_{45}(\mathbf{R}(\text{ci456})) = E_5(\mathbf{R}(\text{ci456})) - E_4(\mathbf{R}(\text{ci456}))$ and $\Delta E_{56}(\mathbf{R}(\text{ci456}))$ are approximately 400 and 1000 cm^{-1} using CI2 at **R**(ci456) obtained using CI1. The principal changes for **R**(ci456) determined using CI2 are an increase in R(C_1−C_2) by 0.03 Å and an increase in the twisting of the associated terminal CH_2 by 10°. Using CI2 exclusively, $E_x(456) = 6.4$ eV, giving a shift in energy due to differential electron correlation of over twice the 0.2 eV shift observed in the vertical and adiabatic excitation energies. These differences, which do not affect the conclusions of this study, will be the subject of a future work.

3.2.1. 4,5^{2}A and 5,6^{2}A Conical Intersection Seams. As noted previously, the three-state degeneracy can be lifted partially producing a two-state degeneracy in two ways: either the 4,5^{2}A (2^2A_1, 1^2B_2) states remain degenerate or the 5,6^{2}A (2^2B_1, 1^2B_2) states remain degenerate. Because these seams have a state in common, we refer to them as linked seams. The description of these regions is complicated by the fact that the derivative couplings can be double-valued necessitating the introduction of branch cuts for their proper description. Here we report, for the first time, energy minimized sections of a pair of linked seams (Figure 3). A detailed analysis of the derivative couplings in this region will be reported in a future work.

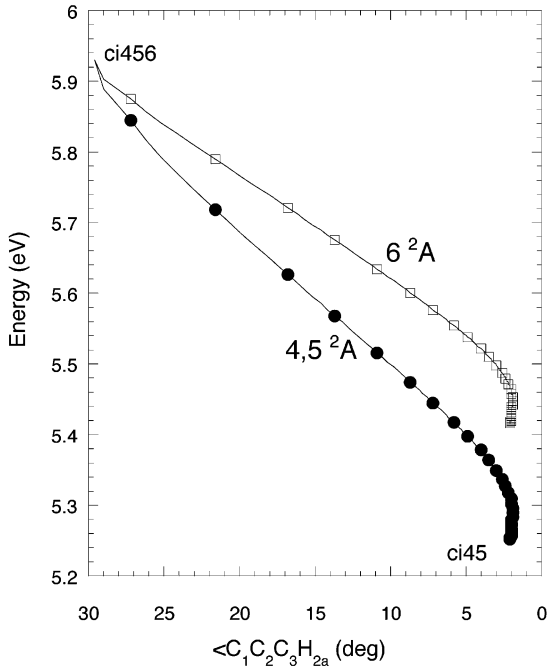

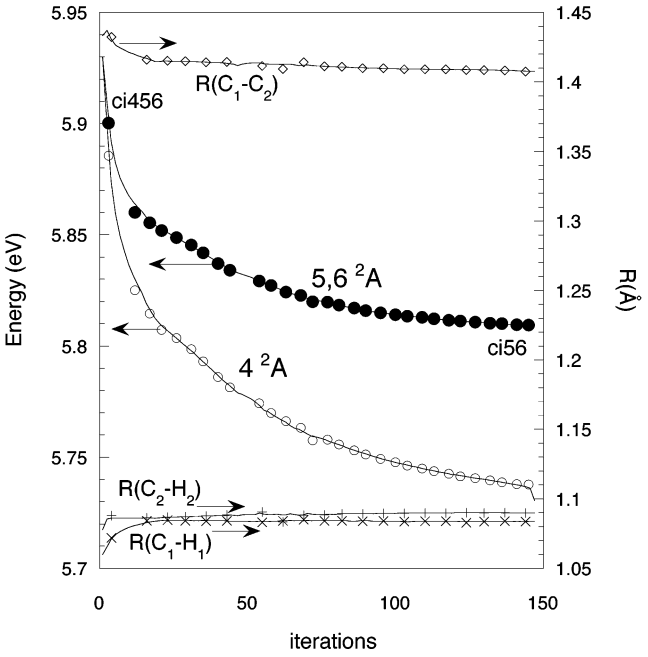

Figure 3. Pathway from a point on the 4,5,6^{2}A seam along the (a) 4,5^{2}A seam and (b) 5,6^{2}A seam. The energies of the three states are shown using CI1. For the 4,5^{2}A seam, the energy is plotted as a function of dihedral angle ∠$C_1C_2C_3H_{2a}$. For the 5,6^{2}A seam, the energy is plotted as a function of iteration number, and select internal coordinates are plotted as well

3.2.1.1. 4,5^{2}A Conical Intersection Seam. Since the pathway on the 4,5^{2}A seam involves rotation of the CH_2 groups toward a planar structure, Figure 3a shows that seam as a function of the dihedral angle ∠$C_1C_2C_3H_{2a}$. The final computed point on the 4,5^{2}A conical intersection seam, ci45, the intersection point with lowest computed energy, is approximately planar, with the

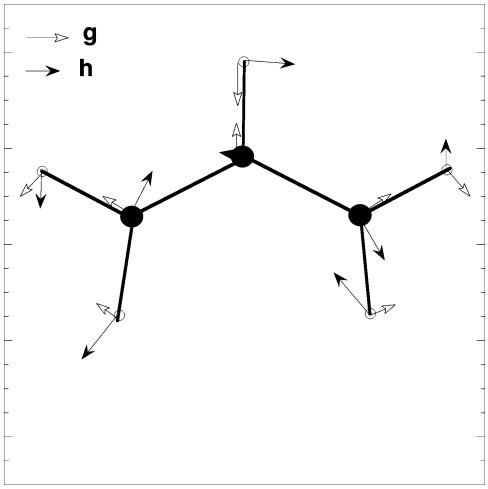

Figure 4. **g** and **h** vectors that span the branching space of the 4,5^{2}A seam. Vectors are scaled for visual clarity.

4,5^{2}A states correlating with the 2^2A_1, 1^2B_2 states. At the CI2 level, $E_x(45)$ is only 0.15 eV higher than $E_5(\mathbf{R}(\text{eql5}))$, the adiabatic excitation energy of the 5^{2}A (1^2B_2) state, and lower than $E_6(\mathbf{R}(\text{eql6}))$ (see Table 2). Thus, the 4,5,6^{2}A seam is connected to a two-state conical intersection seam between the 4,5^{2}A states that includes points with energies comparable to the adiabatic excitation energies.

The 4^{2}A ($\tilde{B}(^2A_1)$) local minimum, eql4, is readily accessible from this region of 4,5^{2}A seam. This can be seen as follows. Near ci45, the 4^{2}A and 5^{2}A states each have (approximately) A′ symmetry. As a consequence, the two vectors, **g** and **h** that span the branching plane,[2] have A′ symmetry (a_1 and b_2 in C_{2v} symmetry) and are shown in Figure 4. When the system is displaced from ci45 along these coordinates, it evolves to eql4 without encountering a barrier.

3.2.1.2. 5,6^{2}A Conical Intersection Seam. Figure 3b shows the 5,6^{2}A seam determined using CI1. The section of the 5,6^{2}A conical intersection seam we were able to locate only lowers the energy by 0.12 eV and retains a nonplanar structure. CI2 calculations confirmed this description of the 5,6^{2}A seam.

Following the discussion in the previous section concerning the importance of correlation in the energies and locations of conical intersections, we notice that ci56, like ci456, exhibits a shift of ca. 0.4 eV in the energy of the conical intersection between CI1 and CI2 results. However, at ci45 the shift is only 0.2 eV. This observation leads us to the conclusion that differential correlation effects are most significant for the 6^{2}A state. Thus, while the qualitative aspects of the topographical features presented here are reliable, the excited state energies are not fully converged with respect to the MRCI description. This is likely the source of the discrepancy in the ordering of the $\tilde{C}$ and $\tilde{D}$ states noted previously. In the future, a more sophisticated treatment of the states in question will be used to refine the predicted energetics.

3.3. 3,4,5^{2}A Conical Intersections. We considered the possibility of three-state degeneracies of the 3,4,5^{2}A states whose adiabatic excitation energies are more disparate. Indeed, three-state intersections were found for these states but at much higher excitation energies, at least 7.37 eV. Ci345 is reported in Table 2. Note the 0.2 eV CI1/CI2 differential correlation for $E_x(345)$, as expected from the above analysis. While too high to be relevant in the recent photochemical studies of the allyl radical, nevertheless, the existence of seams of conical intersections for both 4,5,6 and 3,4,5 states demonstrates that three-state degeneracies are more prevalent than one would anticipate and they should not be ignored when studying the photochemistry of molecules lacking spatial symmetry.

4. Conclusions

Points on a three-state conical intersection seam involving the spectroscopically observed $\tilde{B}$, $\tilde{C}$, and $\tilde{D}$ Rydberg states of the allyl radical have been found. Near the minimum energy portion of this seam, the energy is approximately 0.9 eV above the vertical excitation energy of the $\tilde{D}$ state and the nuclear configuration approximates that of the ground-state structure. In addition, this seam of three-state intersections was shown to be the source of a linked pair of two-state conical intersection seams, one of which approaches the equilibrium geometry of the $\tilde{B}$ state. Thus, this well studied molecule provides a valuable laboratory for the study of "accidental" three-state conical intersections and linked two-state intersections, topographical features that, although having received inadequate attention, may have important implications for nonadiabatic dynamics. It is hoped that these results will motivate experimental and theoretical studies of this question.

Acknowledgment. This work is supported by DoE-BES Grant DEFG0291ER14189 to D.R.Y.

JA036201V